Nuclear Engineering and Technology 54 (2022) 2147–2155

Contents lists available at ScienceDirect

Nuclear Engineering and Technology

journal homepage: www.elsevier.com/locate/net

Original Article

Beyond design basis seismic evaluation of underground liquid storage tanks in existing nuclear power plants using simple method

Shen Wang

Department of Civil Engineering, Shanghai University, Shanghai, 200444, China

ARTICLE INFO

Article history:
Received 26 October 2021
Received in revised form
9 December 2021
Accepted 13 December 2021
Available online 18 December 2021

Keywords:
Underground liquid storage tank
Nuclear safety related
Beyond design basis seismic evaluation
Hand calculation method

ABSTRACT

Nuclear safety-related underground liquid storage tanks, such as those used to store fuel for emergency diesel generators, are critical components for safety of hundreds of existing nuclear power plants (NPP) worldwide. Since most of those NPP will continue to operate for decades, a beyond design base (BDB) seismic screening of safety-related underground tanks in those NPP is beneficial and essential to public safety. The analytical methodology for buried tank subjected to seismic effect, including a BDB seismic evaluation, needs to consider both soil-structure and fluid-structure interaction effects. Comprehensive analysis of such a soil-structure-fluid system is costly and time consuming, often subjected to availability of state-of-art finite element tools. Simple, but practically and reasonably accurate techniques for seismic evaluation of underground liquid storage tanks have not been established. In this study, a mechanics based solution is proposed for the evaluation of a cylindrical underground liquid storage tank using hand calculation methods. For validation, a practical example of two underground diesel fuel tanks in an existing nuclear power plant is presented and application of the proposed method is confirmed by using published results of the computer-aided System for Analysis of Soil Structural Interaction (SASSI). The proposed approach provides an easy to use tool for BDB seismic assessment prior to making decision of applying more costly technique by owner of the nuclear facility.

1. Introduction

There are hundreds of operating nuclear power plants worldwide, majority of which have been in service for more than 30 years and will continue to operate for decades. Nuclear safety-related underground emergency fuel storage tanks are extensively used in aforementioned plants, which are used to supply fuel oil to emergency diesel generators during a Safe Shutdown Earthquake (SSE) (Fig. 1). The design and evaluation of those nuclear safety related underground tanks is generally controlled by seismic loads. During the accident of Fukushima Nuclear Power Plant at 2011, the emergency generator system failed after the combined seismic-tsunami event which led to catastrophic consequences as results of reactor overheat and radiation leakage. Given that many existing nuclear power plants worldwide have similar emergency diesel generator systems, a simpler method for assessing those emergency systems for postulated seismic loads beyond their design basis is valuable. Such effort being performed over a wide span of the nuclear industry shall also include evaluation of hundreds of underground diesel fuel tanks.

Seismic analysis of liquid storage tanks requires consideration of the hydrodynamic forces exerted by the fluid on the tank wall, as a result of seismic excitation. This effect can be well represented by an equivalent mechanical model. Housner [1] was the first to propose such a mechanical model for circular and rectangular rigid tanks, which was later improved by Wozniak and Mitchell [2]. Veletsos and Young [3] used a different approach to develop a similar type of mechanical model for circular rigid tanks. Subsequently, Haroun and Housner [4] and Veletsos [5] developed mechanical models for flexible tanks. The flexible tank model by Veletsos [5] was further simplified by Malhotra et al. [6]. It is also observed by Veletsos [5] that there is no significant difference in the results obtained from rigid and flexible tank models. Design parameters for cylindrical, spherical and ellipsoidal tanks can be found in the literatures by Budiansky [7], Dodge et al. [8], Kana [9], Mccarty et al. [10], Mccarty and Stephens [11], Rattaya [12], Stofan and Armstead [13] and Papaspyrou et al. [14]. Mechanical models described above are widely used by various design codes for liquid storage tank design. ACI 350.3 [15], AWWA D-100 [16], AWWA D-

E-mail address: swang@shu.edu.cn.

https://doi.org/10.1016/j.net.2021.12.016

Nomenclature

a_p, a_s, a_{rp}, a_{rs}	Particle accelerations of P-Wave, S-Wave, R-Wave-P and R-Wave-S, respectively
a_0, a_{0BD}	Design basis and beyond design basis peak seismic accelerations, respectively
a_{ZP}, a_{ZPBD}	Design basis and beyond design basis zero period seismic accelerations, respectively
C_p, C_r, C_s	Propagation velocities of P-Wave, R-Wave and S-Wave, respectively
E'	Modulus of Soil Reaction
E_t	Elastic modulus of tank steel
F_{dyn}	Dynamic seismic force due to liquid acceleration
F_{liquid}	Equivalent static seismic force due to liquid acceleration
h	Embedment depth of the tank
I_{eq}	Moment of inertia per unit length of the tank wall
k_d	Dynamic load factor
L	Tank length
p_{sur}	Surcharge live load
P_{ex}	Static soil pressure on the top of tank
P_w	Equivalent uniform soil pressure
R	Tank radius
t_e	Effective tank shell thickness
ν_m	Poisson's ratio of the soil medium
V_p, V_s, V_{rp}, V_{rs}	Particle velocities of P-Wave, S-wave, R-Wave-P and R-Wave-S, respectively
V_{ZP}, V_{ZPBD}	Design basis and beyond design basis zero period seismic velocities, respectively
W_c, W_i	Convective and impulsive fluid mass, respectively
γ	Total shear strain caused by seismic waves
γ_p, γ_s, γ_{rp}, γ_{rs}	Shear strain caused by P-Wave, S-Wave, R-Wave-P and R-Wave-S, respectively
γ_{pm}, γ_{sm}, γ_{rpm}, γ_{rsm}	Maximum value of γ_p, γ_s, γ_{rp}, γ_{rs}, respectively
nD_1, nD_2, nD_3	Ovaling deflection caused by static load, seismic wave, and accelerated liquid, respectively
ε_a	Total bending strain caused by seismic waves
ε_{ap}, ε_{as}, ε_{arp}	Axial strain caused by P-Wave, S-Wave and R-Wave-P, respectively
ε_{apm}, ε_{asm}, ε_{arpm}	Maximum value of ε_{ap}, ε_{as}, ε_{arp}, respectively
ε_b	Total bending strain caused by seismic waves
ε_{bp}, ε_{bs}, ε_{brp}, ε_{brs}	Bending strain caused by P-Wave, S-Wave, R-Wave-P and R-Wave-S, respectively
ε_{bpm}, ε_{bsm}, ε_{brpm}, ε_{brsm}	Maximum value of ε_{bp}, ε_{bs}, ε_{brp}, ε_{brs}, respectively
ρ_l	Density of contained liquid
ρ_s	Density of soil medium
σ_x^{max}	Maximum total longitudinal stress
σ_{x2}^{max}, σ_{x3}^{max}	Maximum longitudinal stress induced by seismic wave and accelerated liquid, respectively
σ_y^{max}	Maximum total hoop stress
σ_{y1}^{max}, σ_{y2}^{max}, σ_{y3}^{max}	Maximum hoop stress due to static loads, seismic wave, and accelerated liquid, respectively
∇_1	Deflection lag factor
∇_2	Bedding constant

110 [17] and API 650 [18] adopt mechanical model by Housner [1] with modification of Wozniak and Mitchell [2]. Guideline [19] by New Zealand National Society for Earthquake Engineering (NZSEE) use mechanical model of Veletsos and Young [3] for rigid tanks and the one by Haroun and Housner [4] for flexible tanks. Eurocode 8 [20] suggests the models of Veletsos and Young [3] and Housner [1] for rigid circular and rigid rectangular tanks, respectively. For flexible tanks, the models of Veletsos [5] and Haroun and Housner [4] are recommended by Eurocode 8 [20] along with the procedure of Malhotra et al. [6]. However, design methods provided in aforementioned codes and literatures exclusively focus on ground supported or elevated liquid storage tanks and thus are not appropriate for evaluation of underground liquid storage tanks.

Fig. 1. Underground emergency fuel tank.

On the other hand, methods used for seismic analysis of underground structures (conduits, tunnels, and wall casings, etc) are available in various literatures such as Shah and Chu [21], Hall and Newmark [22], Hindy and Novak [23], O'Rourke and Wang [24], Bulson [25], Moser [26], American Lifeline Alliance [27] and Hashash et al. [28,29]. Those methodologies are occasionally adopted for underground liquid storage tank design, neglecting the hydrodynamic forces excited by seismic, which on the contrary is considered as a major mechanism of concern in cases of above-ground liquid storage tank design.

There is no hand calculation method currently available for underground liquid storage tank design considering both soil-structure and fluid-structure interaction effects. Advanced simulation techniques and finite element analysis tools are generally used for this purpose. However, such analysis is often subject to availability of state-of-art finite element tools, which are costly and time consuming. A simple and practically accurate mechanics based solution for the evaluation of cylindrical underground liquid storage tanks is presented in this paper. The proposed approach provides an easy to use tool for BDB seismic evaluation of underground emergency fuel storage tanks in existing nuclear power plants worldwide, compared to more costly technique can be made by owner of the nuclear facility.

The underground liquid storage tank considered here is shown in Fig. 2 with an embedment depth of h (from the top of tank to the ground elevation) and oriented with its axis in the horizontal direction; R and t_e denote radius and effective thickness respectively of the cylindrical section of the underground tank. A global coordinate system is established such that X, Y and Z represent longitudinal, transverse, and vertical directions, respectively. A design basis seismic excitation may be applied at any arbitrary incident angle. A local coordinate system is established for the cylindrical section such that x, y and z represent longitudinal, hoop (tangential) and radial directions, respectively. Hoop stress σ_y and longitudinal stress σ_x within the cylindrical shell of the tank, during a seismic event, is of primary interest of this paper.

A static analysis is conducted first based on Spangler's method and closed-form shell theory for calculation of the shell stresses caused by overburden pressure combined with internal pressure due to liquid weight. Second, the analysis of the seismic load on the underground tank is decoupled into two steps. Step 1 focuses on the effect of seismic waves on the underground tank shell. The soil pressure on the tank caused by traveling seismic waves is analyzed by using a closed form free field solution. In step 2, the seismic load related to acceleration of contained liquid and its effect on tank wall has been analyzed by using a proposed equilibrium approach.

A practical example concerning two underground diesel fuel tanks in an existing nuclear power plant is presented. The proposed mechanical formulae are validated for Design Basis (DB) seismic load case via published results of a computer-aided Soil-Structure Interaction (SSI) analysis using SASSI. Furthermore, the proposed method is used to evaluate those underground tanks subjected to a Beyond Design Bases (BDB) seismic event.

2. Static analysis

Consider the cylindrical underground liquid storage tank shown in Figs. 2 and 3, the overburden pressure on the top of the tank causes ovaling and generates significant moment, which is the main concern in the static analysis of a buried structure [25]. [26]. [27]. Use Spangler's method, the static ovaling deflection or diameter change of the tank ΔD_1 is given by [26].

$$\Delta D_1 = \frac{2R\nabla_1\nabla_2 P_{ex}}{E_t I_{eq}\big/R^3 + 0.061E'} \tag{1}$$

Where $\nabla_1 = 1.0 \sim 1.5$ and $\nabla_2 = 0.1$ are the deflection lag factor and the bedding constant, respectively; P_{ex} is the overburden pressure on the top of the tank caused by soil weight $\rho_s gh$ and surcharge live load p_{sur}, with load factors appropriately assigned to; E_t denotes the elastic modulus of the tank; $I_{eq} = t_e^3/12$ is moment of inertia per

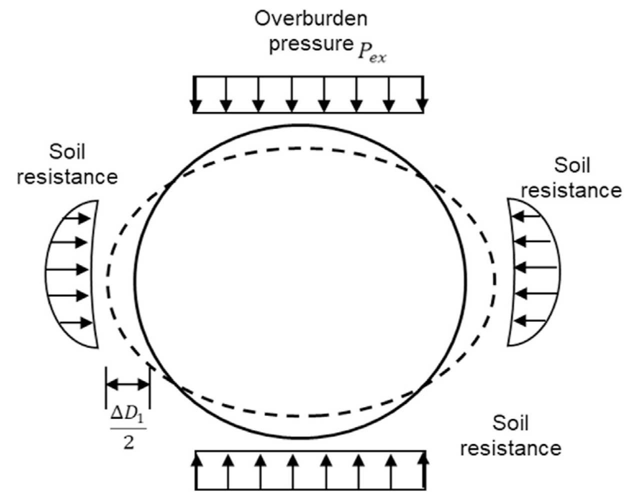

Fig. 3. Ovaling of the underground tank due to static overburden.

unit length of the tank wall; E' represents the modulus of soil reaction. Values of E' vary from close to zero for dumped, loose, fine-grained soil to 3000 psi for highly compacted, coarse-grained soil. Many researchers have attempted to correlate the physical meaning of the modulus of soil reaction E' with other soil properties. The most common parameter used in these efforts is the constrained modulus which is the soil stiffness under three-dimensional strain [26]. In engineering practice, Table 1 may be used to obtain the modulus of soil reaction under different soil conditions [26].

Soil type 1: Fine-grained soils (LL > 50), soils with medium to high plasticity CH, MH, CH-MH.

Soil type 2: Fine-grained soils (LL < 50), soils with medium to no plasticity CL, ML, ML-CL with less than 25% coarse-grained particles.

Soil type 3: Fine-grained soils (LL < 50), soils with medium to no plasticity CL, ML, ML-CL with more than 25% coarse-grained particles. Coarse-grained soils with fines. GM, GC, SM, SC contain more than 12% fines.

Soil type 4: Coarse-grained soils with little or no fines. GW, GP, SW, SP contain less than 12% fines.

Soil type 5: Crushed rock.

With ovaling deflection ΔD_1 calculated from Eq. (1), the maximum static through-wall bending hoop stress σ_{y11}^{max} due to the static overburden pressure is then obtained by Ref. [27]:

$$\sigma_{y11}^{max} = E_t \cdot \frac{\Delta D_1}{R} \cdot \frac{t_e}{R} \tag{2}$$

In the static analysis of the liquid storage tank, the internal

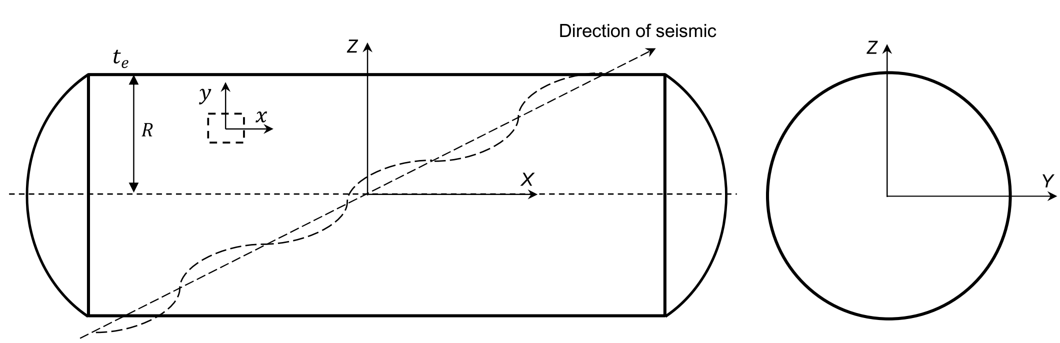

Fig. 2. Underground liquid storage tank.

Table 1
Values of modulus of soil reaction E′ [26].

Soil Type	E′ for degree of soil compaction			
	Dumped	Slight compaction	Moderate compaction	High compaction
1	No data available, consult a competent soils engineer; otherwise, use E′ = 0			
2	50 psi (0.345 MPa)	200 psi (1.38 MPa)	400 psi (2.76 MPa)	1000 psi (6.90 MPa)
3	100 psi (0.69 MPa)	400 psi (2.76 MPa)	1000 psi (6.90 MPa)	2000 psi (13.8 MPa)
4	200 psi (1.38 MPa)	1000 psi (6.90 MPa)	2000 psi (13.8 MPa)	3000 psi (20.7 MPa)
5	1000 psi (6.90 MPa)	3000 psi (20.7 MPa)	3000 psi (20.7 MPa)	3000 psi (20.7 MPa)

pressure load caused by the weight of stored fuel in the tank also needs to be considered. The closed-form solutions of maximum tank hoop stresses σ_{y12}^{max} caused by internal liquid pressure are given by Ref. [30]:

$$\sigma_{y12}^{max} = \begin{cases} \dfrac{2\rho_l g R^2}{t_e}, for\ \ a\ \ full\ \ tank \\ \dfrac{\rho_l g R^2}{t_e}, for\ \ a\ \ half\ \ tank \end{cases} \tag{3}$$

In which $\rho_l g$ represents unit weight of stored liquid.

Immediately, the maximum hoop stress σ_{y1}^{max} due to static loads follows from Eq. (2) and Eq. (3) as

$$\sigma_{y1}^{max} = \sigma_{y11}^{max} + \sigma_{y12}^{max} \tag{4}$$

3. Effect of seismic waves on tank wall

The seismic analysis of the underground liquid storage tank is conducted in two steps. Step 1 focuses on the effect of seismic waves on the underground tank wall excluding contained liquid. In step 2, the seismic effects due to acceleration of contained liquid including sloshing effect is analyzed.

In this section, the effect of seismic waves on the underground tank wall is analyzed using the widely accepted free field solution, neglecting effects of contained liquid. Maximum longitudinal stress σ_{x2}^{max}, and maximum hoop stress σ_{y2}^{max} within the cylindrical shell induced by seismic wave effect are discussed below.

In the free field solution, it is assumed that ground strains caused by seismic waves are in the absence of structures or excavations. The assumption that relative motion between the buried structure and the surrounding soil is negligible has been shown by O'Rourke and Wang [24] to be a valid assumption for most practical cases.

The expressions for axial, bending and shear strains of the underground cylindrical structure are given by Ref. [28]:

$$\varepsilon_{ap}(\phi) = \frac{V_p}{C_p}\cos^2\phi \quad \text{and} \quad \varepsilon_{apm} = \frac{V_p}{C_p} \tag{5}$$

$$\varepsilon_{as}(\phi) = \frac{V_s}{C_s}\cos\phi\sin\phi \quad \text{and} \quad \varepsilon_{asm} = \frac{V_s}{2C_s} \tag{6}$$

$$\varepsilon_{arp}(\phi) = \frac{V_{rp}}{C_r}\cos^2\phi \quad \text{and} \quad \varepsilon_{arpm} = \frac{V_{rp}}{C_r} \tag{7}$$

$$\varepsilon_{bp}(\phi) = \frac{Ra_p}{{C_p}^2}\cos^2\phi\sin\phi \quad \text{and} \quad \varepsilon_{bpm} = 0.385\frac{Ra_p}{{C_p}^2} \tag{8}$$

$$\varepsilon_{bs}(\phi) = \frac{Ra_s}{{C_s}^2}\cos^3\phi \quad \text{and} \quad \varepsilon_{bsm} = \frac{Ra_s}{{C_s}^2} \tag{9}$$

$$\varepsilon_{brp}(\phi) = \frac{Ra_{rp}}{{C_r}^2}\cos^2\phi\sin\phi \quad \text{and} \quad \varepsilon_{brpm} = 0.385\frac{Ra_{rp}}{{C_r}^2} \tag{10}$$

$$\varepsilon_{brs}(\phi) = \frac{Ra_{rs}}{{C_r}^2}\cos^2\phi \quad \text{and} \quad \varepsilon_{brsm} = \frac{Ra_{rs}}{{C_s}^2} \tag{11}$$

$$\gamma_p(\phi) = \frac{V_p}{C_p}\cos\phi\sin\phi \quad \text{and} \quad \gamma_{pm} = \frac{V_p}{2C_p} \tag{12}$$

$$\gamma_s(\phi) = \frac{V_s}{C_s}\cos^2\phi \quad \text{and} \quad \gamma_{sm} = \frac{V_s}{C_s} \tag{13}$$

$$\gamma_{rp}(\phi) = \frac{V_{rp}}{C_r}\cos\phi\sin\phi \quad \text{and} \quad \gamma_{rpm} = \frac{V_p}{2C_p} \tag{14}$$

$$\gamma_{rs}(\phi) = \frac{V_{rs}}{C_r}\cos\phi \quad \text{and} \quad \gamma_{rsm} = \frac{V_{rs}}{C_r} \tag{15}$$

In Eq. (5) thru (15), ϕ denotes angle between the direction of seismic wave propagation and the tank axial orientation; $\varepsilon_{ap}(\phi)$, $\varepsilon_{as}(\phi)$ and $\varepsilon_{arp}(\phi)$ are axial strain of the tank caused by P-Wave (compression wave), S-wave (shear wave) and Rayleigh Wave's compression components (R-Wave-P), respectively; $\varepsilon_{bp}(\phi)$, $\varepsilon_{bs}(\phi)$, $\varepsilon_{brp}(\phi)$ and $\varepsilon_{brs}(\phi)$ are bending strains caused by P-Wave, S-Wave, R-Wave-P and Rayleigh Wave shear components (R-Wave-S), respectively; $\gamma_p(\phi)$, $\gamma_s(\phi)$, $\gamma_{rp}(\phi)$ and $\gamma_{rs}(\phi)$ are shear strains caused by P-Wave, S-Wave, R-Wave-P and R-Wave-S, respectively; ε_{apm}, ε_{asm}, ε_{arpm}, ε_{bpm}, ε_{bsm}, ε_{brpm}, ε_{brsm}, γ_{pm}, γ_{sm}, γ_{rpm} andγ_{rsm} represent maximum values of corresponding strain category with respect to angle ϕ; V_p, V_s, V_{rp} and V_{rs} are respectively the particle velocities of P-Wave, S-Wave, R-Wave-P and R-Wave-S; a_p, a_s, a_{rp} and a_{rs} are respectively the particle accelerations of P-Wave, S-Wave, R-Wave-P and R-Wave-S; C_p, C_s and C_r are respectively the propagation velocities of P-Wave, S-Wave, and Rayleigh Wave.

Note that the propagation velocities C_p, C_s and C_r are soil properties, while the particle velocitiesV_p, V_s, V_{rp}, V_{rs} and the particle accelerations a_p, a_s, a_{rp}, a_{rs} are site-specified seismic characteristics. In practice, values of the zero period velocity V_{ZP} and the zero period acceleration a_{ZP} from Design Basis (DB) and Beyond Design Basis (BDB) seismic response spectrum of the site may be used for the particle velocities and particle accelerations, respectively.

For evaluation purpose, the total axial strain ε_a, bending strain ε_b and shear strain γ are obtained by using SRSS combination of maximum strain caused by various seismic waves as

$$\varepsilon_a = \sqrt{\varepsilon_{apm}{}^2 + \varepsilon_{asm}{}^2 + \varepsilon_{arpm}{}^2} \quad (16)$$

$$\varepsilon_b = \sqrt{\varepsilon_{bpm}{}^2 + \varepsilon_{bsm}{}^2 + \varepsilon_{brpm}{}^2 + \varepsilon_{brsm}{}^2} \quad (17)$$

$$\gamma = \sqrt{\gamma_{pm}{}^2 + \gamma_{sm}{}^2 + \gamma_{rpm}{}^2 + \gamma_{rsm}{}^2} \quad (18)$$

Consequently, the maximum longitudinal stress σ_{x2}^{max} due to effects of seismic wave on the tank is conservatively obtained as:

$$\sigma_{x2}^{max} = E_t(\varepsilon_a + \varepsilon_b) \quad (19)$$

The free field distortion also causes ovaling deformations of the underground tank as shown in Fig. 4.

If the ovaling stiffness of the underground tank is equal to that of the surrounding soil medium, the ovaling deformation can be estimated by neglecting the tank-soil interaction (referred to as "non-perforated case"). On the other hand, if the ovaling stiffness is considerably small compared to the surrounding soil, the ovaling deformation should be estimated by considering the tank-soil interaction (referred as "perforated case"). In most cases of underground liquid storage tanks used in nuclear power plants, perforated assumption should be used. This is also conservative because deformation predicted using perforated assumption is larger than the one using non-perforated assumption.

Considering a perforated case, the free field solution of the ovaling deflection or diameter change of the tank ΔD_2 caused by seismic wave effect is given by [28].

$$\Delta D_2 = 2\gamma(1 - \nu_m) \times 2R \quad (20)$$

with ν_m as Poisson's ratio of the soil medium. For a thin-shell underground tank, the tank shell stress could be conveniently calculated using the formula from Ref. [27] which is developed for underground pipelines. Similar to Eq. (2), with ovaling deflection ΔD_2 calculated from Eq. (20), the maximum through-wall bending hoop stress σ_{y2}^{max} due to the seismic wave on the tank is then obtained by:

$$\sigma_{y2}^{max} = E_t \cdot \frac{\Delta D_2}{R} \cdot \frac{t_e}{R} \quad (21)$$

4. Seismic analysis of contained liquid

The seismic analysis conducted in Section 3 focuses on the effect of seismic waves on the underground tank wall, neglecting contained liquid. The analysis in this section therefore deals with tank stress caused by the accelerated liquid stored within the tank. Mechanical formulae provided in Ref. [1] thru [20] exclusively focus on ground supported or elevated liquid storage tanks thus are not sufficient for evaluation of underground liquid storage tanks. In lieu of using complicated dynamic analysis, a simple method is proposed in this paper using equivalent static concept to evaluate soil-structure-liquid interaction.

Hydrodynamic forces are generated by acceleration of the contained liquid. The pressure associated with these forces can be separated into impulsive and convective parts. The impulsive pressures are associated with inertia forces produced by accelerations on the walls of the container and are directly proportional to these accelerations. The convective pressures are those produced by the oscillations of the fluid. This phenomenal can be well represented by an equivalent mechanical model, in which impulsive part of the liquid is rigidly fastened to the tank walls while the convective part is connected to the tank wall either by springs or as a pendulum. The tank-liquid system is demonstrated in Fig. 5.

As shown in Fig. 5, the convective fluid mass W_c is connected to the tank by the spring with stiffness k_c, and the impulsive fluid mass W_i is rigidly connected to the tank. W_c, W_i and k_c can be calculated using the suitable approach available in several design codes and literatures as discussed in Section 1. Note that these parameters depend only on the tank shape, liquid properties and free surface elevation, but not the characteristics of excitation imposed on the tank.

In order to combine the impulsive and convective forces, Eurocode 8 [20] recommend use of absolute summation rule while other design codes [15]. [16]. [17]. [18] suggest SRSS rule. In the paper, the absolute summation rule is adopted for conservatism. Thus the dynamic seismic force on the tank wall due to liquid acceleration F_{dyn} is given by:

$$F_{dyn} = a_c W_c + a_i W_i \quad (22)$$

In which a_c and a_i are seismic accelerations for impulsive fluid mass and convective fluid mass, respectively. Seismic accelerations a_c and a_i are determined from the seismic response spectrum upon the natural period for the corresponding single degree of freedom (SDOF) comprised of mass (W_c or W_i) and stiffness (k_c or rigid link). A conservative alternative adopted in this paper, is to use peak seismic acceleration a_0 (note $a_0 \geq a_c$ and $a_0 \geq a_i$) from the power plant's design spectrum.

$$F_{dyn} = a_0(W_c + W_i) \quad (23)$$

Note that the solution of Eq. (23) is applicable for seismic load in axial, vertical and transverse directions because difference between

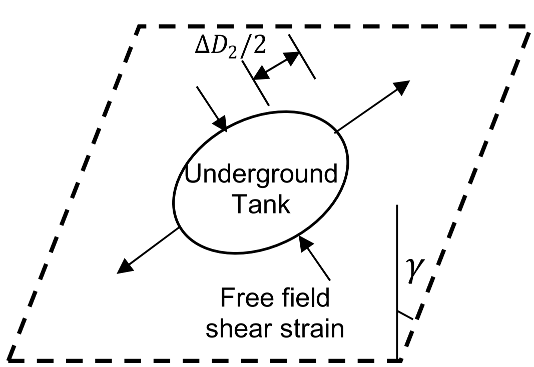

Fig. 4. Ovaling of the underground tank due to free field shear distortion.

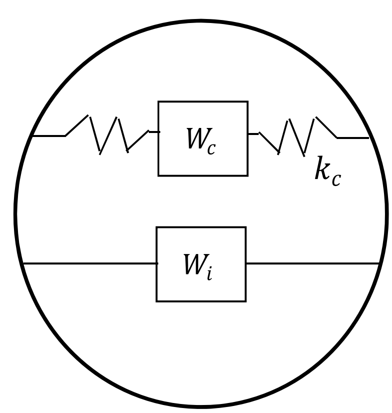

Fig. 5. Tank-liquid system.

the convective fluid mass W_c and the impulsive fluid mass W_i is eliminated. It is also demonstrated in Eq. (23) that the critical inertial seismic force F_{dyn} will always occur when the tank is completely filled.

The next step is to determine maximum hoop stress σ_{y3}^{max} and maximum longitudinal stress σ_{x3}^{max} caused by the liquid seismic force F_{dyn}. In lieu of using complicated dynamic analysis considering soil-structure-liquid interaction, a simple method is proposed in this paper using equivalent static concept. The equivalent static seismic force on the tank shell F_{liquid} due to accelerated liquid may be obtained from F_{dyn} multiplied by the dynamic load factor k_d as:

$$F_{liquid} = k_d F_{dyn} \tag{24}$$

In practice, k_d could be assumed as $k_d = 2.0$ for most cases of tank design. Per Housner's approach, one can assume the total liquid inertial force F_{liquid} is equally divided and applied on both sides of the tank and balanced by lateral soil pressure force F_{soil} (i.e., $F_{soil} = F_{liquid}$) in the direction of applied seismic load. The seismic excitation may occur at any incident angle as shown in Fig. 2. Thus the seismic load at X direction which causes longitudinal stress σ_x, and the seismic load in YZ plane which generating hoop stress σ_y are considered respectively in Fig. 6a and Fig. 6b. Note that soil friction is neglected for simplicity. This approximation is conservative because it increases the magnitude of soil pressure force F_{soil}, which leads to larger stresses in tank shell.

As shown in Fig. 6a, the maximum longitudinal stress σ_{x3}^{max} in the cylindrical shell caused by acceleration of contained liquid is given by an equilibrium solution as:

$$\sigma_{x3}^{max} = \frac{F_{liquid}}{4\pi R t_e} \tag{25}$$

For the analytical case with the seismic load in YZ plane as shown in Fig. 6b, ovaling deformation will be caused by the combination of liquid inertial force F_{liquid} and lateral soil force F_{soil}, and resisted by soil pressure in orthogonal direction as shown in Fig. 7.

The liquid inertial force F_{liquid} and lateral soil force F_{soil} demonstrated in Fig. 7 are in fact distributed pressure rather than concentrated force. Therefore as an engineering approximation, a uniform pressure P_w is adopted to substitute F_{liquid} as shown in Fig. 8.

The soil pressure P_w is given by

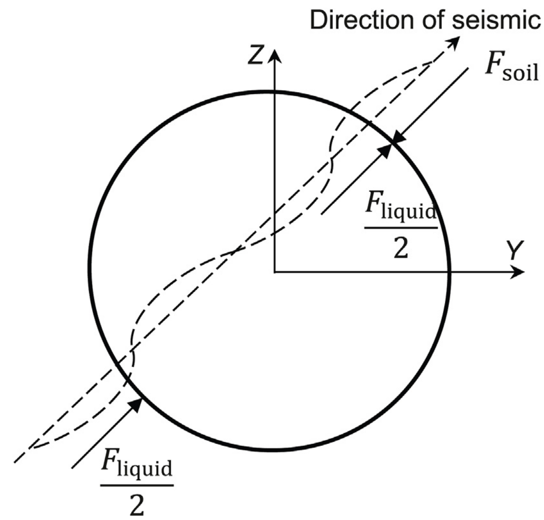

Fig. 6b. Equilibrium of tank-liquid-soil system: seismic load in YZ plane.

$$P_w = \frac{F_{liquid}}{4RL} \tag{26}$$

With L is the length of the tank. Fig. 8 is similar to the model demonstrated in Fig. 3, Spangler's method can be used to solve the

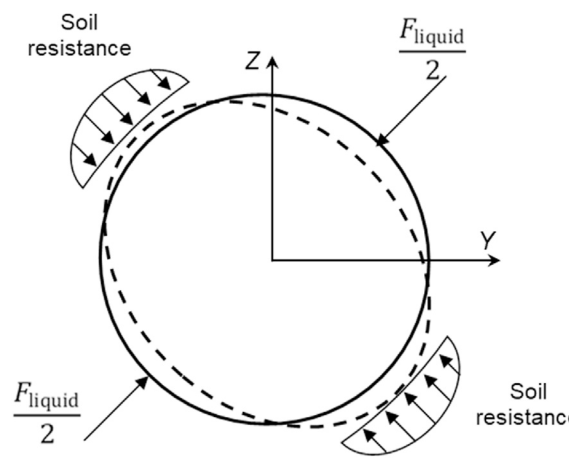

Fig. 7. Ovaling due to liquid inertial force.

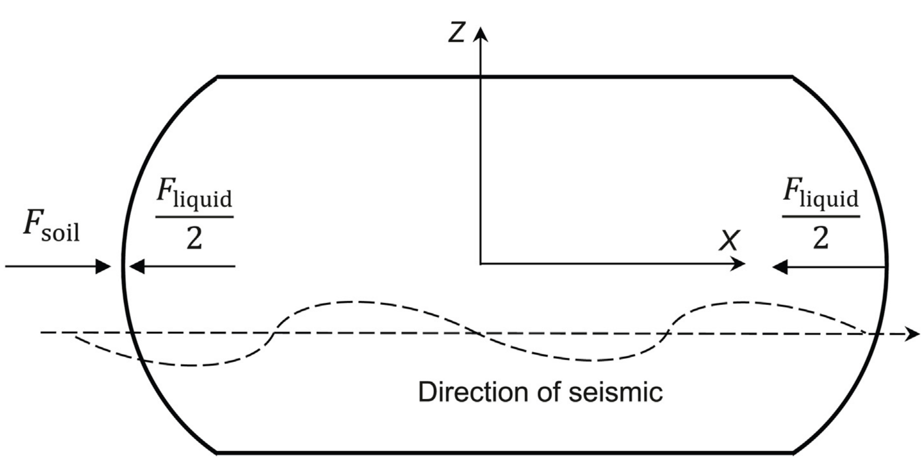

Fig. 6a. Equilibrium of tank-liquid-soil system: seismic load in X direction.

tank ovaling deflection ΔD_3 and corresponding maximum hoop stress σ_{y3}^{max} due to accelerated liquid as per References [26,27]:

$$\Delta D_3 = \frac{2R\nabla_1\nabla_2 P_w}{E_t I_{eq}/R^3 + 0.061E'} \tag{27}$$

$$\sigma_{y3}^{max} = E_t \cdot \frac{\Delta D_3}{R} \cdot \frac{t_e}{R} \tag{28}$$

Also see Eq. (1) and Eq. (2) for definition of parameters.

5. Evaluation of underground cylindrical liquid storage tank

The evaluation of the underground liquid storage tank is conducted by using stresses obtained in aforementioned formulas against the suitable design code. Note that during a seismic event, the seismic excitation could be imposed at any incident angle. Thus the maximum stresses originating from individual loads may occur at the same location within the tank shell. For example, σ_{y1}^{max} and σ_{y3}^{max} may occur simultaneously when a seismic excitation propagates in vertical direction, as demonstrated by Figs. 2 and 7. Therefore, it is recommended that the combined maximum stresses in hoop direction σ_{y}^{max} and the combined maximum stress in longitudinal direction σ_{x}^{max} should be conservatively obtained using absolute summation rule as:

$$\sigma_{y}^{max} = \sigma_{y1}^{max} + \sigma_{y2}^{max} + \sigma_{y3}^{max} \tag{29}$$

$$\sigma_{x}^{max} = \sigma_{x2}^{max} + \sigma_{x3}^{max} \tag{30}$$

As a summary, the maximum hoop stress σ_{y}^{max} and the maximum longitudinal stressσ_{x}^{max} within the cylindrical shell of the underground liquid storage tank are calculated using following steps:

(1) Obtain design inputs
(2) Calculate the maximum hoop stress due to static load σ_{y1}^{max} using Eq. (4)
(3) Calculate the maximum longitudinal stress due to effects of seismic wave on the tank σ_{x2}^{max} using Eq. (19)

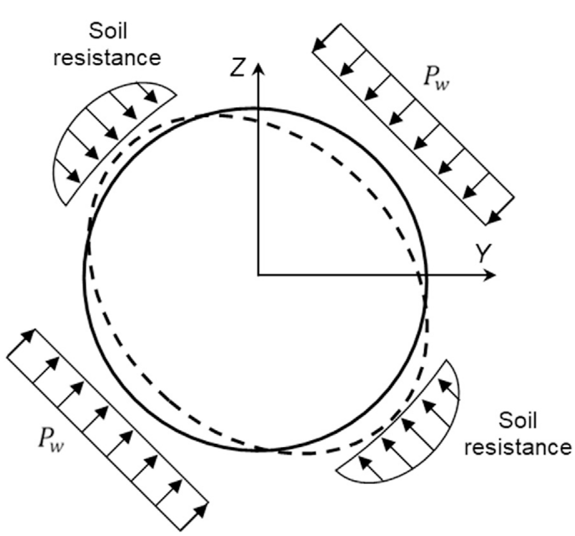

Fig. 8. Ovaling due to equivalent uniform pressure.

(4) Calculate the maximum hoop stress due to effects of seismic wave on the tank σ_{y2}^{max} using Eq. (21)
(5) Calculate the maximum longitudinal stress due to acceleration of contained liquid σ_{x3}^{max} using Eq. (24)
(6) Calculate the maximum hoop stress due to acceleration of contained liquid σ_{y3}^{max} using Eq. (28)
(7) Calculated the combined maximum hoop stress and the combined maximum longitudinal stress using Eq. (29) and Eq. (30)

Although aforementioned formula and processes are developed for a cylindrical underground liquid storage tank oriented with its axis in the horizontal direction, the principle of the proposed method could be easily extended to underground tanks in other geometrical categories.

6. Illustrative example

For validation, a practical example of two underground diesel fuel tanks in an existing nuclear power plant is presented in this section. The application of the proposed method is confirmed by using published results of the computer-aided SASSI analysis.

A series of seismic SSI analyses of two new replacement diesel fuel steel tanks at Diablo Canyon Nuclear Power Plant was carried out and published by Deng et al. [31]. Two-Dimensional (2D) and Three-Dimensional (3D) models were established using the computer program SASSI, including tank, surrounding soil and contained fuel. It is found in seismic analyses by Deng et. Al. [31]. that a full tank always exerts larger seismic force in the tank shell compared to a half-full tank. This is consistent with the discussion related to Eq. (3) and Eq. (23). A full tank condition is thus considered in this example herein.

Design inputs including tank dimensions, soil properties and site-specified seismic characters are provided by Deng et al. [31] and summarized in Table 2.

In order to carry out a practical example, parameters are determined in Table 3 using references and formulas presented in previous sections.

Following Step (2) -Step (7), design basis seismic results of maximum hoop stresses and longitudinal stresses within the cylindrical shell of the tank are calculated in Table 4. Also included in Table 4 are corresponding results using 2D and 3D SASSI models per Deng et al. [31].

As shown in Table 4, the maximum hoop stress σ_{y}^{max} predicted using the proposed simple hand calculation method show good agreement with the ones obtained from SASSI analyses, with differences less than 5%. In the case of maximum longitudinal stress, σ_{x}^{max} calculated using the proposed method is 20% higher than the one predicted by 3D SASSI model. Conservatism with such magnitude is deemed to be acceptable for the evaluation of nuclear safety related structures.

With proposed formula validated by SASSI results, beyond design basis seismic results of maximum hoop stresses and longitudinal stresses within the cylindrical shell of the tank are calculated in Table 5. As shown in Table 5, the beyond design basis seismic stress of Diablo Canyon Diesel Fuel Tanks are as high as 61.5 ksi in longitudinal direction, which may raise concern for further evaluation.

As a summary, it is demonstrated in this example that the proposed simple hand calculation method is capable to assess an underground liquid storage tank with reasonable accuracy. The results could serve as preliminary data points in the early stage evaluation before a comprehensive finite element analysis is conducted, or as an independent check for the result obtained from the

Table 2
Design inputs for diablo canyon diesel fuel tanks [31].

Parameters	Description
$R = 6.0$ ft (1.83 m)	Tank radius
$t_e = 0.5$ in (12.7 mm)	Effective tank shell thickness, excluding outer layer to account for future damage
$L = 65$ ft (19.8 m)	Tank length
$h = 8$ ft (2.44 m)	Embedment depth from top of the tank to the ground elevation
$\nu_m = 0.4$	Poisson's ratio of the soil medium
$C_s = 3000$ ft/s (914 m/s)	Soil shear wave (S-Wave) propagation velocity
$a_0 = 2.2\ g$	Design basis peak seismic acceleration, note $g = 9.81$ m/s^2 represents gravity acceleration
$a_{ZP} = 0.7\ g$	Design basis zero period seismic acceleration
$a_{0BD} = 3.7\ g$	Beyond design basis peak seismic acceleration, defined as 1.67 times of design basis value per [32]
$a_{ZPBD} = 1.2\ g$	Beyond design basis zero period seismic acceleration, defined as 1.67 times of design basis value per [32]
$\rho_s g = 140$ pcf (22 kN/m^3)	Unit weight of soil medium

Table 3
Parameters determined for Diablo Canyon Diesel Fuel Tanks.

Parameters	Description	Reference
$\rho_l g = 55$ pcf (8.64 kN/m^3)	Unit weight of diesel fuel	Per Westbrook [33]
$E' = 1000$ psi (6.9 MPa)	Modulus of Soil Reaction	Per Diablo Canyon FSAR [34] and Table 1.
$E_t = 29000$ ksi (2.0×10^5 MPa)	Elastic modulus of steel	
$\nabla_1 = 1.25$	Deflection lag factor	Per [26,27]
$\nabla_2 = 0.1$	Bedding constant	Per [26,27]
$p_{sur} = 150$ psf (7.2 KPa)	Surcharge live load	Per Diablo Canyon FSAR [34]
$P_{ex} = 11$ psi (76 KPa)	Static soil pressure on the top of tank	Calculated as $P_{ex} = 1.2\rho_s gh + 1.6p_{sur}$, with 1.2 and 1.6 are load factors
$V_{ZP} = 33.6$ in/s (0.85 m/s)	Design basis zero period seismic velocity	Calculated as $V_{ZP} = 48a_{ZP}/g$ per Mohraz and Sadek [35]: Table 2–9.
$V_{ZPBD} = 56.1$ in/s (1.42 m/s)	Beyond design basis zero period seismic velocity	Calculated as $V_{ZPBD} = 48a_{ZPBD}/g$ per Mohraz and Sadek [35]: Table 2–9.
$C_p = 7350$ ft/s (2240 m/s)	P-Wave propagation velocity	Calculated as $C_p = C_s\sqrt{\frac{2-2\nu_m}{1-\nu_m}}$ per Hashash et al. [28] where ν_m is the Poisson's ratio of the soil medium
$C_r = 3000$ ft/s (914 m/s)	Rayleigh Wave propagation velocity	Conservatively using the propagation velocity of S-Wave
$W_c + W_i = 402$ kipm (1.8×10^5 kg)	Total mass of liquid for a full tank	Calculated as $W_c + W_i = \rho_l \pi R^2 L$

finite element analysis.

7. Conclusion

In the wake of 2011 Fukushima Nuclear Plant catastrophic event, design of emergency generator system in existing nuclear power plants are subjected to scrutiny for postulated seismic loads, within or even beyond their design basis. There is a need for evaluating design of hundreds of underground diesel fuel tanks, which have been widely used in nuclear industry for decades.

There is no simple method currently available for underground tank design considering both soil-structure and fluid-structure interaction effects. Advanced simulation techniques and finite element analysis tools are occasionally used for this purpose. However, such analysis is often subject to availability of state-of-art finite element tools, as well as costly and time consuming.

In this paper, a simple, but practically and reasonably accurate mechanical based solution has been proposed, in order to evaluate an underground liquid storage tank for static and seismic loads. A practical example concerning two underground diesel fuel tanks in an existing nuclear power plant is presented. The proposed hand calculation method is implemented for both design basis and beyond design basis seismic loads. The design basis results are validated by comparing with published results of a computer-aided SSI analysis using SASSI. The beyond design basis results can be used to evaluate those underground tanks subjected to a BDB seismic event.

The proposed solution could be applied in beyond design basis

Table 4
Design basis seismic results of Diablo Canyon Diesel Fuel Tanks.

	Maximum Hoop Stress	Maximum Longitudinal Stress
Mechanical formulae	$\sigma_y^{max} = 16.3$ ksi (112 MPa)	$\sigma_x^{max} = 36.9$ ksi (254 MPa)
2D SASSI model [31]	$\sigma_y^{max} = 16.5$ ksi (114 MPa)	Not available in 2D analysis
3D SASSI model [31]	$\sigma_y^{max} = 17$ ksi (117 MPa)	$\sigma_x^{max} = 30$ ksi (227 MPa)

Table 5
Beyond design basis seismic results of Diablo Canyon Diesel Fuel Tanks.

	Maximum Hoop Stress	Maximum Longitudinal Stress
Mechanical formulae	$\sigma_{yBD}^{max} = 20.8$ ksi (144 MPa)	$\sigma_{xBD}^{max} = 61.5$ ksi (424 MPa)

evaluation of hundreds of existing cylindrical underground liquid storage tank. The proposed approach provides an easy to use tool for BDB seismic evaluation prior to making decision of applying more costly technique. The principle of the proposed solution could also be used to develop solutions for other tank for which soil-tank-liquid interaction need to be taken into consideration.

Declaration of competing interest

The authors declare that they have no known competing financial interests or personal relationships that could have appeared to influence the work reported in this paper.

References

[1] G.W. Housner, Dynamic Pressure on Fluid Containers, TID 7024 (Chapter 6) and Appendix, F, US Atomic Energy Commission, 1963.

[2] R.S. Wozniak, W.W. Mitchell, Basis of seismic design provisions for welded steel oil storage tanks, in: American Petroleum Institute 43rd Midyear Meeting, Session on Advances in Storage Tank Design, Canada, Toronto, 1978.

[3] A.S. Veletsos, Young, Earthquake response of liquid storage tanks, in: Proc. Of 2nd Engg. Mechanics Specialty Conf, ASCE Raleigh, 1977, pp. 1–24.

[4] M.A. Haroun, G.W. Housner, Seismic design of liquid storage tanks, J. Tech. Counc. ASCE 107 (No. TC1) (1981) 191–207.

[5] A.S. Veletsos, Seismic response and design of liquid storage tanks, in: Guidelines for Seismic Design of Oil & Gas Pipelines System, ASCE, NY, 1984, pp. 255–370.

[6] P.K. Malhotra, T. Wenk, M. Wieland, Simple procedure for seismic analysis of liquid storage tanks, Structural Engineering, IABSE 10 (No.3) (2000) 197–201.

[7] B. Budiansky, Sloshing of liquids circular canals and spherical tanks, J. Aero. Sci. 27 (1960) 161–173.

[8] F.T. Dodge, D.D. Kana, H.N. Abramson, Liquid surface oscillations in longitudinally excited rigid cylinders, AIAA J. 3 (1965) 685–695.

[9] D.D. Kana, An experimental study of liquid surface oscillations in longitudinally excited compartmented cylindrical and spherical tanks, NASA CR- 545 (1966).

[10] J.L. Mccarty, H.W. Leonard, W.C. Walton, Experimental investigation of the natural frequencies of liquids in toroidal tanks, NASA TN D-531 (1960).

[11] J.L. Mccarty, D.G. Stephens, Investigation of the natural frequencies of fluids in spherical and cylindrical tanks, NASA TN D-252 (1960).

[12] J.V. Rattaya, Sloshing of liquids in axisymmetric ellipsoidal tanks, AIAA Paper (1965) 65–114.

[13] A.J. Stofan, A.L. Armstead, Analytical and experimental investigation of forces and frequencies resulting from liquid sloshing in a spherical tank, NASA, TN D-1281 (1962).

[14] S. Papaspyrou, S.A. Karamanos, Valougeorgis, Response of half-full horizontal cylinders under transverse excitation, J. Fluid Struct. 19 (2004) 985–1004.

[15] ACI 350.3. Seismic Design of Liquid Containing Concrete Structures and Commentary (ACI 350.3-06), American Concrete Institute, Farmington Hills, MI, 2006.

[16] AWWA D-100, Welded Steel Tanks for Water Storage, American Water Works Association, Colorado, 1996.

[17] AWWA D-110, Wire- and Strand-Wound Circular, Prestressed Concrete Water Tanks, American Water Works Association, Colorado, 1995.

[18] API 650, Welded Storage Tanks for Oil Storage, American Petroleum Institute Standard, Washington D. C, 1998.

[19] M.J.N. Priestley, et al., Seismic Design of Storage Tanks, Recommendations of a Study Group of the New Zealand, National Society for Earthquake Engineering, 1986.

[20] Eurocode 8, Design Provisions for Earthquake Resistance of Structures, Part 1-General Rules and Part 4 – Silos, Tanks and Pipelines, European committee for Standardization, Brussels, 1998.

[21] H.H. Shah, S.L. Chu, Seismic analysis of underground structural elements, Journal of the Power Division of ASCE 100 (No. P01) (1974) 53–62. July.

[22] W.J. Hall, N.M. Newmark, Seismic design for pipelines and facilities, Journal of the Technical Council on Lifeline Earthquake Engineering of ASCE, No. TC1 (1978) 91–107. November.

[23] A. Hindy, M. Novak, Earthquake Response of Underground Pipelines, GEOT-1-1978, Faculty of Engineering Science, University of Western Ontario, London, Ontario, Canada, 1978.

[24] M. O'Rourke, L.R. Wang, Earthquake response of buried pipelines, in: Proceedings of the ASCE Geotechnical Engineering Division Specialty Conference on Earthquake Engineering and Soil Dynamics, Pasadena, California, 1978, pp. 720–731. June 19-21.

[25] P.S. Bulson, Buried Structures – Static and Dynamic Strength, Chapman & Hall, London, 1985.

[26] A.P. Moser, Buried Pipe Design, second ed., McGraw-Hill, 2001.

[27] ALA (American Lifeline Alliance), Guideline for the Design of Buried Steel Pipe, An ASCE and FEMA sponsored study, 2001.

[28] Y.M.A. Hashash, J.H. Hook, B. Schmidt, J.I. Yao, Seismic design and analysis of underground structures, Tunn. Undergr. Space Technol. 16 (2001) 247–293.

[29] Y.M. Hashash, D. Park, J.I. Yao, Ovaling deformations of circular tunnels under seismic loading, an update on seismic design and analysis of underground structures, Tunn. Undergr. Space Technol. 20 (2005) 435–441.

[30] W. Flugge, Stresses in Shells, second ed., Springer-Verlag, 1973.

[31] Deng, N. et. al., Seismic qualification of new underground diesel fuel tanks at the diablo canyon nuclear power plant site, Proceeding of ASME PVP Conference, July 27-31, 1997, Orlando, Florida.

[32] USNRC, NUREG/CR 7253 Technical Considerations for Seismic Isolation of Nuclear Facilities, 2019.

[33] S.R. Westbrook, Fuels for Land and Marine Diesel Engines and for Non-aviation Gas Turbines, MNL1-8TH, ASTM, 2010.

[34] Diablo canyon power plant units 1& 2, final safety analysis report, Rev. 11 (1996).

[35] A. Mohraz, F. Sadek, Earthquake ground motion and response spectra, in: Farzad Naeim (Ed.), Chapter 2 of Seismic Design Handbook, 2001.